**Original Research**

# Brain Diffusivity in Patients with Neuropsychiatric Systemic Lupus Erythematosus with New Acute Neurological Symptoms

Robert C. Welsh, PhD,[1]* Habib Rahbar, BS,[1] Bradley Foerster, MD,[1] Majda Thurnher, MD,[2] and Pia C. Sundgren, MD, PhD[1]

**Purpose:** To investigate the source of significant difference in apparent diffusion coefficient (ADC) between patients with acute symptoms of neuropsychiatric (NP) systematic lupus erythematosus (SLE) (NPSLE) and normal controls.

**Materials and Methods:** Diffusion-weighted echo-planar imaging was performed on 1.5-T scanners in 17 female and four male NPSLE patients with acute neurological symptoms (23–76 years, mean = 42.7 years), and in 21 aged-matched healthy controls (16 female, five male, 26–63 years, mean = 41.1 years). ADC histograms were calculated for whole brain, gray matter tissue, and white matter tissue.

**Results:** Of the 17 NPSLE patients, 13 (72%) had abnormal findings on MR imaging. The NPSLE patients had a mean ADC value of $(1105.1 \pm 23.6) \times 10^{-6}$ mm$^2$/second and the control had a mean ADC value of $(1012.5 \pm 9.4) \times 10^{-6}$ mm$^2$/second ($P \leq 0.0012$). Significant differences were also found in white matter ($P \leq 0.0020$) and gray matter ($P \leq 0.0022$).

**Conclusion:** ADC histogram analysis demonstrated increased general diffusivity in the brain in NPSLE patients with acute symptoms compared with healthy normal controls. This finding suggests that in the brain parenchyma of NPSLE patients a loss of tissue integrity occurs facilitating motility of free-water protons.

**Key Words:** DWI; NPSLE; ADC; histogram; lupus
**J. Magn. Reson. Imaging 2007;26:541–551.**


NEUROPSYCHIATRIC (NP) systemic lupus erythematosus (SLE) (NPSLE) occurs in 25% to 70% of patients with lupus and is associated with increased morbidity and mortality (1). The clinical manifestations of NPSLE include psychosis, stroke, and epilepsy, in addition to more subtle symptoms such as headache and neurocognitive dysfunction (2). Patients with concomitant antiphospholipid antibodies (APL-ab) are at additional risk for neuropsychiatric events. Lupus patients are also at increased risk for a wide range of central nervous system (CNS) events related to immunosuppressive therapy, including infection and drug toxicity, hypercoagulability, and accelerated atherosclerosis.

CNS vasculitis and/or cerebritis represent a potentially severe form of NPSLE and may present with seizures, movements disorders, altered consciousness, stroke, and coma (3). While CNS inflammation is uncommon in SLE, the clinician nevertheless must entertain this diagnosis any time a lupus patient presents with CNS signs or symptoms. Although clinical assessment is the keystone in the diagnosis of NPSLE, the diagnosis is often difficult and remains presumptive in some patients. MR imaging findings are variable and in some cases the MRI is unremarkable (4–9).

Lately, by using advanced techniques as proton MR spectroscopy, single photon emission CT (SPECT), T2 relaxometry, and magnetization transfer imaging (MTI), cerebral abnormalities are found in patients with NPSLE who present with diffuse symptoms. Diffusion-weighted imaging (DWI) is another technique that can depict cerebral abnormalities when conventional MRI fails to do so. DWI is a well established method that is implemented as a part of routine protocol at many institutions around the world. DWI measures the diffusivity of visible water molecules (10) and the principles for the measurement of diffusion with magnetic resonance imaging (MRI) are well described (11,12). DWI has shown to be a very useful tool for early signs of ischemia (13,14) before changes are present on conventional T2-weighted or fluid attenuation inversion recovery (FLAIR) images, but is also increasingly used in the evaluation of other brain diseases, e.g., multiple sclerosis (15–17), trauma (18,19), brain tumor (20,21), and hypertensive encephalopathy (22,23), among others. Histogram analysis of apparent diffusion coefficient (ADC) values in brain of multiple sclerosis patients have illustrated significant differences compared to normal controls (25,26). A recent study has demonstrated the use of volumetric quantitative DWI analysis in NPSLE

[1]Department of Radiology, University Hospital of Michigan, Ann Arbor, Michigan, USA.
[2]Department of Radiology, Vienna University Hospital, Vienna, Austria.
*Address reprint requests to: R.C.W., Department of Radiology, Basic Radiological Sciences Division, Kresge III, Room 3315, 200 Zina Pitcher Place, Ann Arbor, MI 48109-0553. E-mail: rcwelsh@med.umich.edu
Received March 7, 2006; Accepted May 3, 2007.
DOI 10.1002/jmri.21036
Published online in Wiley InterScience (www.interscience.wiley.com).

patients with diffuse symptoms (24). They demonstrated higher ADC values and significantly lower and broader ADC histograms in the NPSLE patients with diffuse, but no acute, clinical symptoms (e.g., no focal or regional signal abnormalities on diffusion weighted images) compared to normal controls (24). We hypothesized that cerebral changes in NPSLE patients with acute new onset of neurological symptoms might be detectable and quantifiable by the means of ADC histogram analysis.

The aim of the present study was to investigate whether volumetric quantitative DWI analysis can depict cerebral abnormalities in patients with acute symptoms of NPSLE and if significant differences in measured whole-brain ADC histograms between these patients and normal controls exist. Additionally, we investigate the ADC distributions in white matter only and gray matter only to further the understanding of observed whole-brain ADC distribution differences.

## MATERIALS AND METHODS

### *Patients*

A total of 21 patients (17 female, four male), aged 23–76 years, mean = 42.7 years, were included in this prospective study. Patients were included if they: 1) fulfilled the 1982 Revised criteria for SLE set forth by the American Rheumatism Association (27); and 2) had new onset of neurological symptoms suspected to be related to their known SLE within a week prior to the initial examination. All patients underwent conventional MR of the brain within 24 hours of admission to the hospital. Follow-up MRI examinations in a limited number of patients were performed three and six months after the initial study. All work that was related to this research was performed in accordance with our institutional review boards and with the expressed informed consent of the participants. Of the 21 patients, 11 (11 female, 0 male) were seen at the first site, and the remaining 10 patients (six female, four male) were scanned at the second site. One of the patients from the second site (female) demonstrated a large lesion on MR imaging and was subsequently removed from further analysis. The remaining 20 patients are reported here.

A group of 21 (16 female, five male) aged-matched normal controls were used for comparison. All of the controls were scanned at the first site.

### *MR Imaging*

The MR examinations were performed on a 1.5-T scanner (GE Medical Systems) at the first site and on a 1.5-T scanner (Philips Medical System) at second site. The conventional MRI examination included: pre- and post-contrast-enhanced axial and sagittal T1-weighted images, axial T2-weighted images with fat saturation, axial FLAIR and DWI images (spin-echo echo-planar imaging [SE-EPI]; $b$ = 1000 seconds/mm$^2$; in three directions: slice, frequency, and phase-encode, combined on the scanner to produce isotropically-weighted DWI and T2-weighted images), and post-contrast-enhanced T1-weighted images in the coronal projection. A total of 20 mL of Gd-diethylene triamine pentaacetic acid (DTPA) (Magnevist, Berlex Laboratories, USA) was intravenously injected before post-contrast-enhanced images.

The MR images were evaluated for brain volume loss (none, mild, moderate, or severe), abnormal signal, abnormal contrast enhancement, abnormal diffusion, presence of hemorrhage or mineralization, and any additional abnormalities. Brain lesions were either classified as infarct-like (moderate to large-sized, roughly wedge-shaped areas of increased T2/FLAIR intensity, and/or encephalomalacia involving gray and white matter) or white matter lesions (further categorized as subcortical, deep, periventricular, punctate, or patchy). Lesions were further characterized as to location and number. Serial imaging was evaluated to characterize lesions as stable, improving, or progressing. Diffusion-weighted images were examined for areas of restricted or increased diffusion, with ADC maps utilized

Clinical data for each patient was extracted via a focused search of our institution's computerized data record, including patient demographics (age, sex, and race), disease characteristics (primary and secondary diagnoses, duration of diagnosis, medications, and presence of APL-ab, clinical symptoms, neurological diagnosis, pathologic diagnosis, therapy, and clinical course.

Summary demographics and clinical characteristics of the 20 patients entered into the study are presented in Table 1. Presenting symptoms for each patient were classified according to the 1999 American College of Rheumatology Nomenclature and Case Definitions for Neuropsychiatric Lupus Syndromes (3) and are summarized in Table 2.

### *DWI and ADC*

Whole-brain ADC histograms were calculated in all subjects (patients and normal controls). To remove regions outside of the brain, as well as removing contributions from the cerebellum, masks (referred to as the "cortical mask") were drawn for each subject using a MATLAB tool. The ADC was calculated in the remaining regions according to $ADC = \log(I_o/I_b)/b$, where $I_0$ is the non-diffusion-weighted T2 ($b$ = 0 seconds/mm$^2$) image and $I_b$ is the diffusion-weighted image with weighting $b$ = 1000 seconds/mm$^2$. Due to the nature of this study, individual diffusion-weighted images (slice, frequency, and phase) were not extracted from the scanner, only the combined isotropically-weighted image and $b$ = 0 seconds/mm$^2$ image. However, both sites undergo routine careful quality assurance for eddy current compensation. As a post hoc test of residual distortion and potential subject motion, DWI images were affine corrected to the T2-weighted image using McFlirt (28). All affine matrices illustrated less than 1% distortion on average in the DWI images. Subject motion was much less than a voxel in any given direction. Given these results, ADC images were calculated from the non-affine-corrected data.

To explicitly remove cerebrospinal fluid (CSF), a small region of interest (ROI) was drawn in the ventricles of each subject's $b$ = 0 seconds/mm$^2$ image (T2). The mean value of this ROI was used to determine a thresh-

Table 1
Patient Demographics*

| Patient number | Gender | Age (years) | Race | Diagnosis | Duration[a] | APL+/APL−[b] |
|---|---|---|---|---|---|---|
| 1 | Female | 45 | W | SLE | 16 years | − |
| 2 | Female | 46 | W | SLE | 20 years | − |
| 3 | Female | 32 | W | SLE | 23 years | − |
| 4 | Female | 59 | AA | SLE | >5 years | + |
| 5 | Female | 44 | AA | SLE | >5 years | + |
| 6 | Female | 52 | W | SLE | 14 years | + |
| 7 | Female | 41 | W | SLE+Sjogren | 10 years | + |
| 8 | Female | 55 | W | SLE+Sjogren | >10 years | − |
| 9 | Female | 23 | As | SLE | 6 month | + |
| 10 | Female | 45 | AA | SLE | 19 years | − |
| 11 | Female | 46 | W | SLE+Sjogren | 13 years | + |
| 12 | Male | 76 | W | SLE | >5 years | + |
| 13 | Female | 62 | W | SLE+Sjogren | 32 years | − |
| 14 | Male | 31 | W | SLE | 12 years | NA |
| 15 | Female | 29 | W | SLE | 3 years | − |
| 16 | Female | 39 | W | SLE | 1 years | NA |
| 17 | Male | 29 | W | SLE | 18 years | − |
| 18 | Female | 46 | W | SLE | >3 years | − |
| 19 | Female | 28 | W | SLE+Sjogren | >3 years | + |
| 20 | Male | 37 | W | SLE | >3 years | + |

*Patient demographics including diagnosis, duration of disease, and presence or absence of antiphospholipid antibodies (APL-Ab). Patients 4, 7, and 10 were excluded from spectroscopy statistics as final clinical diagnosis did not confirm NPSLE.
[a]Duration of disease at the time of the initial MRI study.
[b]Presence of antiphospholipid antibodies (APL-Ab) (+/−).
AA = Afro-American, As = Asian, W = white., NA = not applicable.

old (85% of mean CSF value in the $b = 0$ ROI) to further define a CSF mask (the "csf-exclusion-mask"), as previously done by Bosma et al (24). This was performed subject-by-subject. Finally, the T2 image (the $b = 0$ seconds/mm$^2$ image of the DWI sequence) was segmented (29) into gray, white, and CSF compartments using the segmentation routines in SPM99. By segmenting this T2 image, the resulting gray, white, and CSF segments are, by definition, coregistered to the ADC image. The segmentation results in three probability likelihood images: 1) the likelihood that a voxel is gray matter; 2) the likelihood that a voxel is white matter; and 3) the likelihood that a voxel is CSF. Gray matter (the "gray mask") and white matter (the "white mask") masks were initially constructed using a conservative threshold of 0.85 on the likelihood value. A combined whole "brain mask" was mathematically defined as the intersection of the cortical mask, the csf-exclusion mask, and the union of the gray mask and white mask. To further investigate any differentiation between gray matter diffusion and white matter diffusion, two additional masks were constructed: 1) a "gray only mask" being the intersection of the cortical mask, the csf-exclusion mask, and the gray mask; and 2) a "white only mask" being the intersection of the cortical mask, the csf-exclusion mask, and the white mask.

An issue to address is partial volume effects. Due to the finite spatial sampling inherent in any imaging technique, voxels can be of mixed tissue type, i.e., containing mainly a single tissue type but a fraction may be CSF. That is, if a gray matter voxel contained a fraction of gray matter ($f_{Gray}$) with a diffusion value of $ADC_{Gray}$ and $f_{CSF}$ of CSF with a diffusion value of $ADC_{CSF}$, the observed ADC value in that voxel would be:

$$ADC_{Obs} = f_{Gray} \cdot ADC_{Gray} + f_{CSF} \cdot ADC_{CSF}.$$

Given that the ADC of CSF is 2 to 3 times that of gray matter, then an increased effective value of ADC would be observed for a gray matter voxel that contains a fraction of CSF. To investigate if previously observed increases (24) in ADC are due to partial voluming of CSF, a further refinement of tissue definition was imposed. To further the definition of gray matter and white matter, a "neighborhood-like" function was evaluated for each voxel: a tissue was classified by its likelihood due to segmentation as well as the likelihood classification of its nearest neighbors. The resulting neighborhood-like value ranged from 0 (no like neighbors) to 26 (all like neighbors). Hence, a gray matter voxel surrounded by more gray matter voxels will have less partial volume effects and contribute more cleanly to a measure of gray matter diffusivity, likewise for a white matter voxel. Given that white matter is bulky, we can expect a white matter voxel to exhibit more like neighbors than a gray matter voxel.

Whole-brain histograms, gray matter only histograms, and white matter only histograms were calculated for each subject. These histograms were normalized to unit area. The mean ADC, the width (standard deviation [SD]) of the ADC distributions, the left to right distribution (skewness), and how extended the histogram was (kurtosis) was evaluated in each subject. Group averages and standard errors of these metrics were then calculated across subjects. A $P$ value $< 0.05$ was set for statistical significance using Student's $t$-test.

Table 2
Clinical Symptomology*

| Patient number | Clinical symptoms | Medical treatment | Interval change in symptoms | Final diagnosis |
|---|---|---|---|---|
| 1 | Dysphasia, blurred vision | Methylprednisolone, prednisone 40-20 mg | Improved | Unclear etiology most likely lupus cerebritis |
| 2 | Transient double vision | None | Improved | Ischemic event, lupus cerebritis |
| 3 | Acute left weakness | Methylprednisolone | Improved | Lupus cerebritis |
| 4 | Mental status decline, increased tremor | Multiple medications. No additional medication | Improved | Drug related symptoms |
| 5 | Cognitive dysfunction, history of seizures | None | Unchanged | Lupus cerebritis |
| 6 | Headache | Hydroxychloroquine, dehydroepiandosterone | Improved | Lupus cerebritis |
| 7 | Disorientation, headache | None | Unchanged | Dissociative fugue, conversion disorder, |
| 8 | Increased tremor, tics, diplopia | Prednisone | Improved | Lupus cerebritis |
| 9 | Headache, nephritis, | Cytophosphamide methylprednisolone | Improved | Lupus cerebritis |
| 10 | Syncope, headache, difficulties in finding words | Multiple medications. No additional medication | Improved | Orthostatics |
| 11 | Severe headache, meningitis | Methylprednisolone, prednisone | Improved | Lupus cerebritis |
| 12 | Disorientation, agitation, | Multiple medications. No additional medication | Improved | Lupus cerebritis |
| 13 | Acute left sided hypesthesia | Prednisolone | Unchanged | Lupus cerebritis |
| 14 | Headache | NA | NA | Unclear etiology most likely lupus cerebritis |
| 15 | Fatigue | NA | NA | Unclear etiology most likely lupus cerebritis |
| 16 | History of seizures | None | Unchanged | Lupus cerebritis |
| 17 | Mild mental status decline | None | Unchanged | Lupus cerebritis |
| 18 | Acute left paresis, headache, dysarthria | Prednisolone | Improved | Lupus cerebritis |
| 19 | Acute left-sided hypesthesia, fatigue, nausea | Methylprednisolone | Improved | Lupus cerebritis |
| 20 | Headache, difficulties finding words | Prednisolone | Improved | Lupus cerebritis |

*Clinical symptoms at time of presentation, medical treatment, and interval change in clinical symptoms and final diagnosis for this event of acute symptoms for the 20 SLE patients.

Histograms by group, SLE, and normal controls were then calculated by averaging the unit-normed histograms across the subjects.

## RESULTS

Based on clinical criteria, 17 out of the 20 SLE patients were classified as NPSLE at the final diagnosis. As this study concerns patients with acute onset of NPSLE, the results are dealing only with these 17 patients and 21 controls, except for Tables 1, 2, and 3, which present all 20 of the SLE patients that entered the study. Of the 17 patients, six patients were followed over time and underwent examinations at three and six months as well, and two patients underwent a follow-up study at three months but declined to participate in the final follow-up examination six months after the initial study. All the patients that had follow-up scans were examined at the first site.

Six of the eight patients underwent all three examinations and, therefore, completed the study. Two patients underwent two of the examinations, but declined to participate in the final follow-up examination six months after the initial study. In these eight patients, the cause of their acute symptoms was confirmed as lupus with CNS involvement. In the remaining three patients, who are not included into the proper study of NPSLE, the likely etiology to their symptoms was believed to be drug related (patient 4), orthostatic (patient 10), and dissociative fugue/conversion disorder (patient 7) (Table 2). Seven of the 17 patients were antiphosolipid antibody-positive (APL-ab+) and eight were negative (APL-ab–) (Table 1). In two of the 17 patients no data regarding APL-ab could be found. Of the 17 pa-

Table 3
Clinical MR Findings*

| Patient number | Initial study at time of presentation of symptoms |
|---|---|
| 1 | Normal (0) |
| 2 | Scattered small bilateral nonspecific WM foci, mild brain volume loss (1) |
| 3 | Scattered small foci of signal alterations in WM and GM, moderate brain volume loss (2) |
| 4 | Patchy T2-signal abnormalities in bilateral periventricular WM, abnormal DWI in the left basal ganglia, mild brain volume loss (1), old small infarcts |
| 5 | Scattered small foci of increased T2 signal in bilateral WM (0) |
| 6 | Old well defined smaller infarct left frontal lobe, multiple small scattered areas of increased T2 signal, mild brain volume loss (1) |
| 7 | Mild brain volume loss (1) |
| 8 | Diffuse subcortical and periventricular WM and brainstem signal abnormality, general moderate loss of brain volume (2) |
| 9 | Patchy areas of increased T2 signal in the WM of both hemispheres, petechial hemorrhage (0) |
| 10 | Scattered small foci of increased T2 signal in bilateral WM, small meningioma (0) |
| 11 | Scattered small foci of increased T2 signal in bilateral WM, meningeal enhancement (0) |
| 12 | Patchy areas of increased T2 signal in bilateral WM (0) |
| 13 | Patchy areas of increased T2 signal in bilateral WM, new abnormal DWI +lesions (0) |
| 14 | Normal (0) |
| 15 | Normal (0) |
| 16 | Normal (0) |
| 17 | Normal (0) |
| 18 | Normal (0) |
| 19 | Scattered small foci of increased T2 signal in bilateral WM (0) |
| 20 | Old smaller infarcts bilateral-occipital-parietal, basal ganglia left old defect, new abnormal DWI + lesions (0) |

*Findings at the MRI of the brain in each of the 20 SLE patients entering the study at the initial examination. Patients 4, 7, and 10 were excluded from the final evaluation as described in the main text. Brain loss is indexed in parentheses as: none = 0, mild = 1, moderate = 2, and severe = 3.

tients, 12 (71%) had major neuropsychiatric symptoms, such as cognitive problems, weakness, visual problems, and meningismus. Six patients (29%) had headache and/or mild cognitive complaints, such as difficulties in concentration, memory, or word finding as the only problem at time of the initial study. Morphological brain abnormalities were seen in nine of the 12 patients with major neuropsychiatric symptoms and in four patients with minor neuropsychiatric symptoms on conventional MRI. Eleven patients had some medical treatment for SLE prior to the initial study, most commonly prednisone .

On the whole, 12 of the 17 patients received additional medication after the initial admission; methylprednisolone (five patients), prednisone (six patients), and cyclophosphamide (one patient). The remaining six patients received no additional medication. In the group of eight patients that had additional follow-up MR scanning, seven patients were treated with additional medication after the initial admission: methylprednisolone (four patients), prednisone (two patients), and cyclophosphamide (one patient). The remaining patient received no additional medication. Of the 17 patients with NPSLE, 11 (65%) had clinical response/improvement, whereas six patients (35%) did not improve (Table 2).

### *MR Imaging of the Brain*

Imaging findings are summarized in Table 3. Of the 17 patients, 12 (71%) had abnormal findings on MR imaging. The most common findings were scattered single or multiple foci (seven patients) or patchy areas (four patients) of increased signal on T2-weighted or FLAIR images in the deep and periventricular white matter, with no pathological contrast enhancement. Other abnormal findings included focal foci of increased signal on DWI images, consistent with restricted diffusion in focal acute ischemia (two patients), volume loss or brain atrophy (mild in three and moderate in two patients), old small infarctions (two patients), and meningeal enhancement (one patient). Incidental note was made of small meningiomas in two patients

### *ADC Histograms*

The whole-brain ADC histogram analysis revealed that the NPSLE patients had a mean ADC value of $(1105.1 \pm 23.6) \times 10^{-6}$ mm$^2$/second and the controls a mean value of $(1012.5 \pm 9.4) \times 10^{-6}$ mm$^2$/second. The mean ADC values were significantly higher ($P \leq 0.0012$, two-tailed) in the NPLSE patients compared to the controls. These data are summarized in Figs. 1–4. The group averaged whole-brain (without CSF) ADC histograms are in Fig. 1, clearly illustrating the group differences. The gray matter only and the white matter only ADC histograms for the groups are in Figs. 2 and 3, respectively. The gray matter ADC means, $(1033.6 \pm 24.3) \times 10^{-6}$ mm$^2$/second for NPSLE and $(944.2 \pm 10.8) \times 10^{-6}$ mm$^2$/second for normal controls, are significantly different ($P \leq 0.0022$, two-tailed) between the groups. The white matter only ADC histograms also demonstrated a significance difference in mean ADC values, $(768.6 \pm 10.1) \times 10^{-6}$ mm$^2$/second for NPSLE and $(730.5 \pm 5.3) \times 10^{-6}$ mm$^2$/second for normal controls, ($P \leq 0.0020$, two-tailed). The individual mean ADC val-

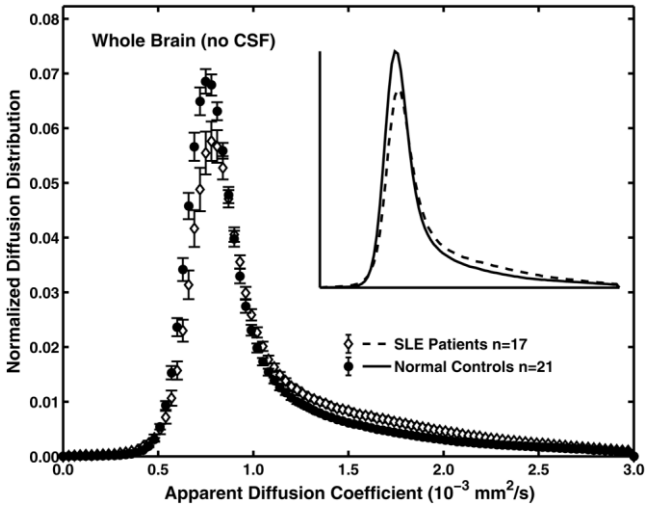


**Figure 1.** Comparison of whole-brain (excluding CSF) ADC histograms between normal controls (filled circles and solid line) and NPSLE patients (open diamonds and dashed line). Standard error bars are calculated from group variance in each histogram bin. Inserts show idealized line plots for clarity of difference away from peak. Histograms are normalized to unit area.

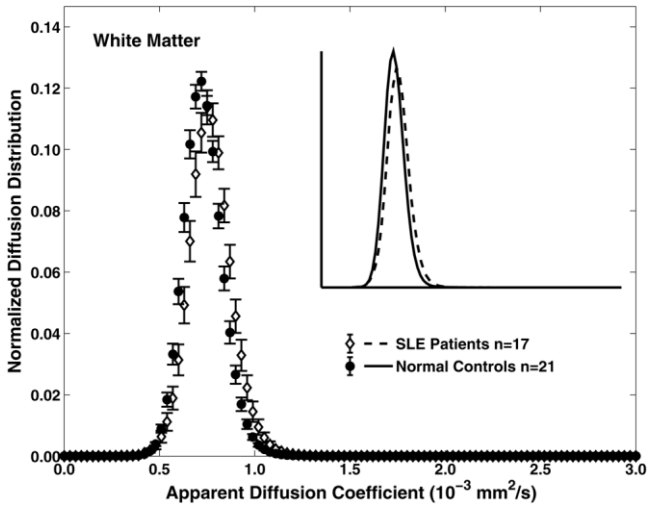


**Figure 3.** Comparison of normal controls (filled circles and solid line) and NPSLE patients (open diamonds and dashed line). Standard error bars are calculated from group variance in each histogram bin. Inserts show idealized line plots for clarity of difference away from peak. Histograms of ADC are for white matter tissue only. No neighborhood-like requirement made. White matter voxel defined by segmentation likelihood value ≥0.85.

ues, as well as the SD of individual ADC histograms, are plotted in Fig. 4. The difference in the widths of the whole-brain ADC distributions between the NPSLE and normal controls stems from differences in the gray matter distributions between the two groups. The significance difference of the widths when examining the whole-brain ADC histograms is $P \leq 0.026$, while in the gray matter it is only $P \leq 0.0068$, and the white-matter only distributions do not appear to have significantly different widths, $P \leq 0.338$.

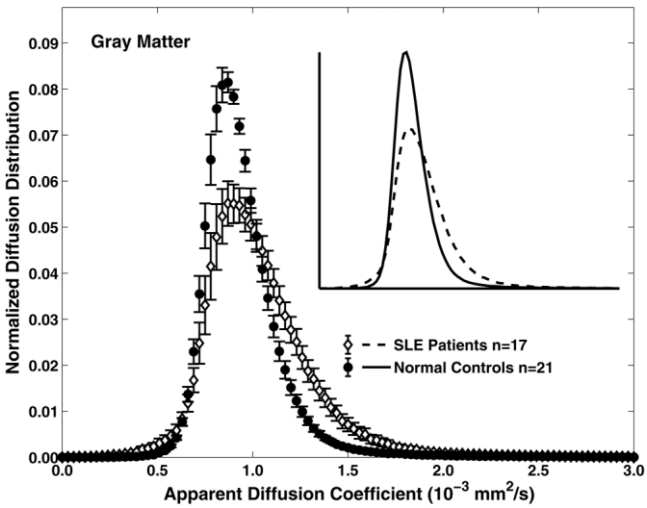


**Figure 2.** Comparison of normal controls (filled circles and solid line) and NPSLE patients (open diamonds and dashed line). Standard error bars are calculated from group variance in each histogram bin. Inserts show idealized line plots for clarity of difference away from peak. Histograms of ADC are for gray matter tissue only. No neighborhood-like requirement made. Gray matter voxel defined by segmentation likelihood value ≥0.85.

To investigate the effect of surrounding tissue (gray, white, or CSF) on the ADC distributions, the neighborhood-like function was used to further refine the definition of white matter and gray matter. Two values of the neighborhood-like function were evaluated for further definition—a value of seven (a moderate constraint on likeness) and a value of 15 (a stringent constraint on likeness). In other words, a voxel of gray matter was only used for the histogram if it had at least seven gray-like neighbors and 15 gray-like neighbors. This criterion was also used for white matter. The resulting ADC histograms for seven neighbors and 15 neighbors are shown in Figs. 5 and 6 for gray matter and white matter, respectively. The individual mean ADC values for each subject are plotted in Fig. 7. As can be seen, the white matter distributions change very little with increasing definition of white matter as determined by the neighborhood-like function. This is mainly due to there being a larger fraction of bulk white matter relative to all white matter in the brain as compared to the fraction of bulk gray matter in the human brain. For a neighborhood-like value of seven, the observed mean gray matter ADC in NPSLE is $(1000.1 \pm 22.1) \times 10^{-6}$ mm$^2$/second, a decrease of approximately 3%. While in the normal controls, the observed ADC mean becomes $(924.9 \pm 10.0) \times 10^{-6}$ mm$^2$/second, a decrease of 2%, there still is a significant difference observed in the ADC means between the two groups ($P \leq 0.0041$). Under the tighter definition of gray matter, using a neighborhood-like value of 15, the difference in ADC means, $(910.6 \pm 17.5) \times 10^{-6}$ mm$^2$/second for NPSLE and $(869.8 \pm 9.5) \times 10^{-6}$ mm$^2$/second for normal controls, is still significant, though much less so, at $P \leq 0.044$. There is

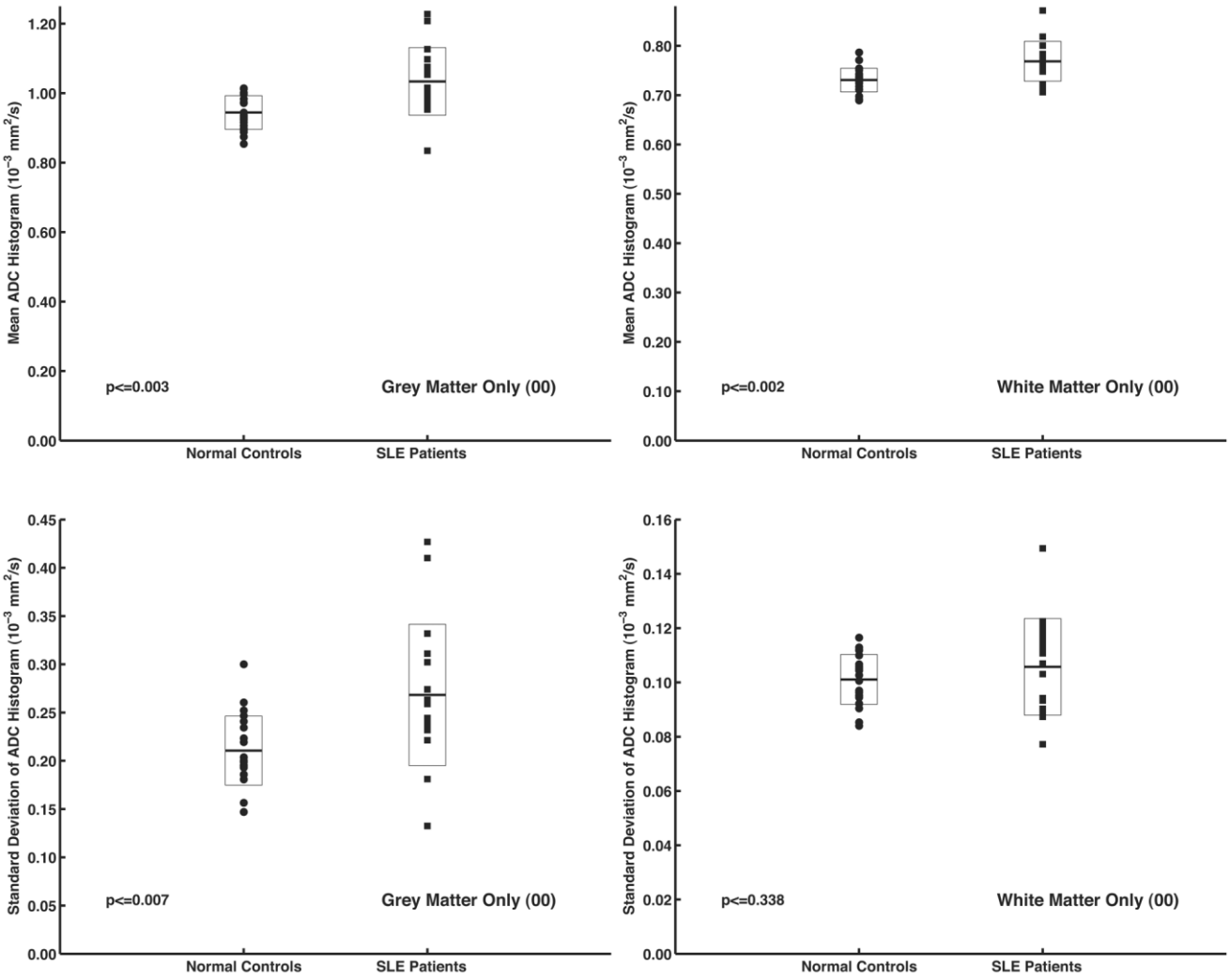


**Figure 4.** Individual mean values of individual ADC histograms and SDs of individual ADC histograms for gray matter and white matter tissue respectively. Boxes indicate ± SD about the group mean.

also still a significant difference ($P \leq 0.0063$) in the widths of the gray matter ADC distributions, (181.3 ± 16.0) × $10^{-6}$ mm$^2$/second for NPSLE and (131.4 ± 5.0) × $10^{-6}$ mm$^2$/second for normal controls.

The neighborhood-like influence on the white matter distributions is less marked, with the NPSLE mean ADC values being (762.9 ± 9.4) × $10^{-6}$ mm$^2$/second and (760.8 ± 9.8) × $10^{-6}$ mm$^2$/second for neighborhood-like values of seven and 15 respectively. For normal controls, the mean white matter ADC value does not change, (729.6 ± 5.3) × $10^{-6}$ mm$^2$/second and (726.1 ± 5.3) × $10^{-6}$ mm$^2$/second for neighborhood-like values of seven and 15, respectively. The two groups maintain significance difference, $P \leq 0.0023$ and $P \leq 0.0026$, for neighborhood-like values seven and 15. Table 4 summarizes these statistical results.

## DISCUSSION

Our results of significantly increased ADC values on whole-brain ADC histograms are in agreement with a previous study (24). It seems that these findings do not only occur in NPSLE patients with diffuse symptoms with no focal or regional signal abnormalities seen on the DWI (24), but also in NPSLE patients with acute onset of neurological symptoms and with, as here presented, signal abnormalities on DWI (two patients) consistent with acute ischemic changes, and, therefore, most likely reflects permanent cerebral alterations seen in this patient group regardless of severity or duration of neurological symptoms. We also observe that these increases in ADC values are found in gray matter only and white matter only, indicating that the cerebral alterations is not limited to one tissue compartment.

It seems less likely that the, in general, small or, in few cases, patchy white matter hyperintensities that were present on the conventional T2-weighted and FLAIR images in some of the patients would be responsible for the significantly different diffusion pattern in NPSLE because they were in general small in number and size. Only in two of the patients were there small foci of restricted diffusion (seen as increased signal on the DWI; $b = 0$ seconds/mm$^2$ image) and not present on the conventional T2-weighted or FLAIR images. This is

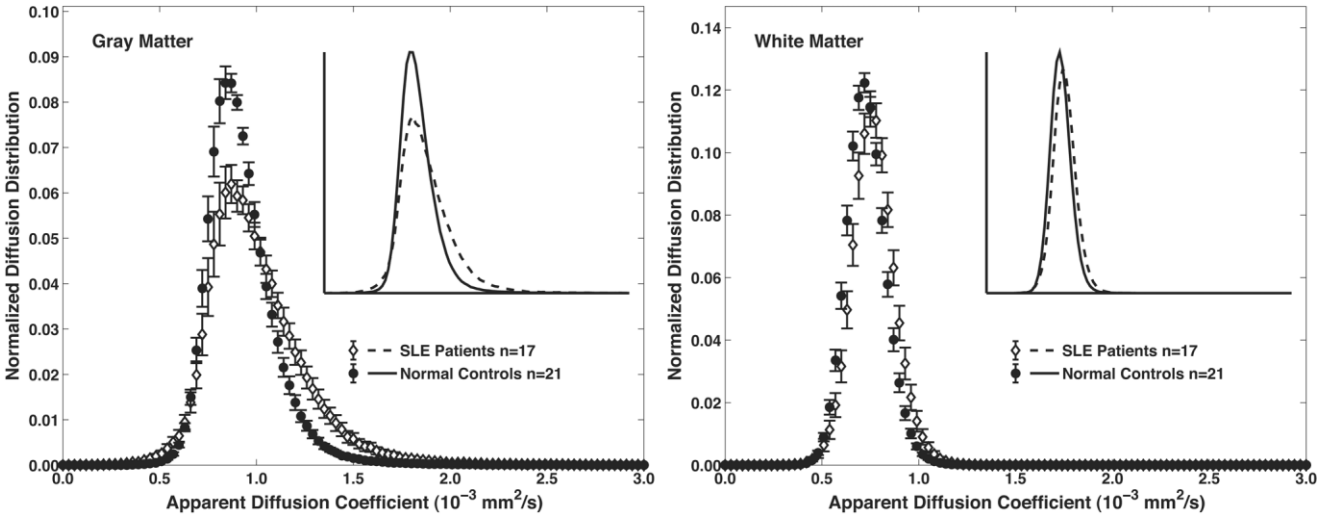


**Figure 5.** Comparison of normal controls (filled circles and solid line) and NPSLE patients (open diamonds and dashed line) gray matter tissue and white matter tissue ADC histograms with increased neighborhood-like function, seven like-neighbors. Standard error bars are calculated from group variance in each histogram bin. Inserts show idealized line plots for clarity of difference away from peak.

a finding consistent with acute ischemia. In addition, to eliminate the possibility of influence of larger CSF volumes or edema, one patient with a large infarct was excluded from the study before any measurements were performed.

It has been suggested that the abnormal findings seen in the brain of NPSLE patients are not related to hypoxic/anaerobic events, but, rather, indicate a host response to injury, such as an inflammatory reaction, membrane activation, or demyelination (30). Such a theory can be supported by histopathology studies in which gliosis and demyelination has been described in the brain parenchyma of patients with NPSLE (31). Vasculopathy, which is a common abnormality described in NPSLE patients (32–34), might lead to altered cerebral blood flow as previously demonstrated with PET and SPECT in NPSLE patients (35–39). An altered cerebral blood flow might lead to metabolic abnormalities and axonal loss and associated demyelination, which have been suggested in MR spectroscopy studies and MTI studies (40–42).

The probability of such a pathogenetic pathway is also supported by the MR spectroscopy findings seen in eight of our 18 NPSLE patients (43). That study demonstrated significant decreased N-acetyl aspartate (NAA)/choline (Cho) ratios with further decrease over time, an interval decrease of NAA/creatinine (Cr) over time, and significantly elevated Cho/Cr and lactate/lipids (LL)/Cr ratio at presentation, with no interval change over time compared to normal controls. The

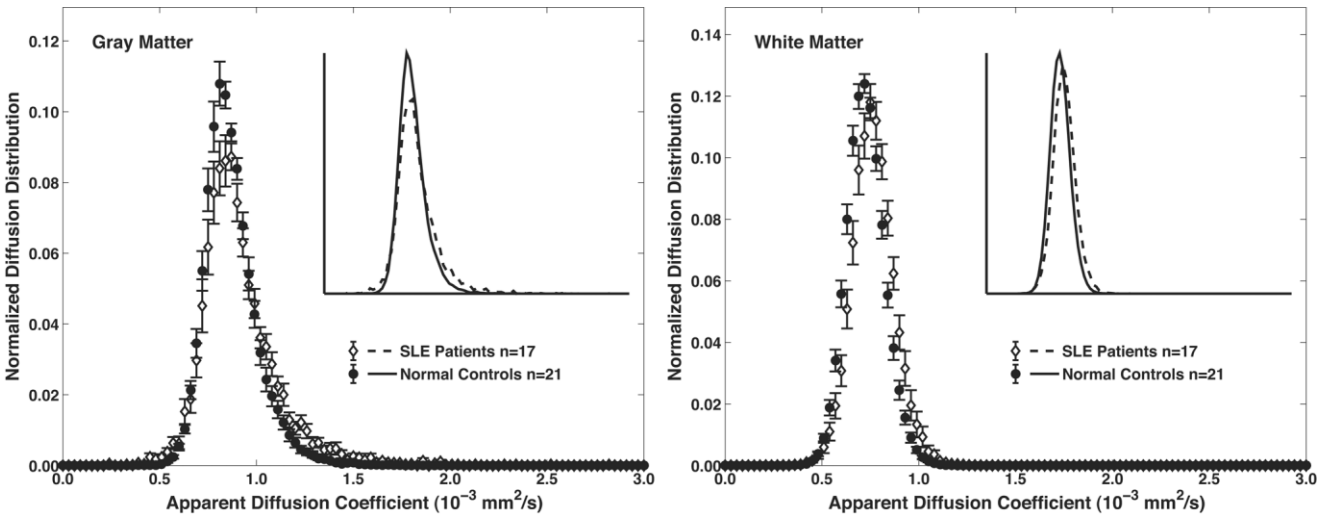


**Figure 6.** Comparison of normal controls (filled circles and solid line) and NPSLE patients (open diamonds and dashed line) gray matter tissue and white matter tissue ADC histograms with increased neighborhood-like function, 15 like-neighbors. Standard error bars are calculated from group variance in each histogram bin. Inserts show idealized line plots for clarity of difference away from peak.

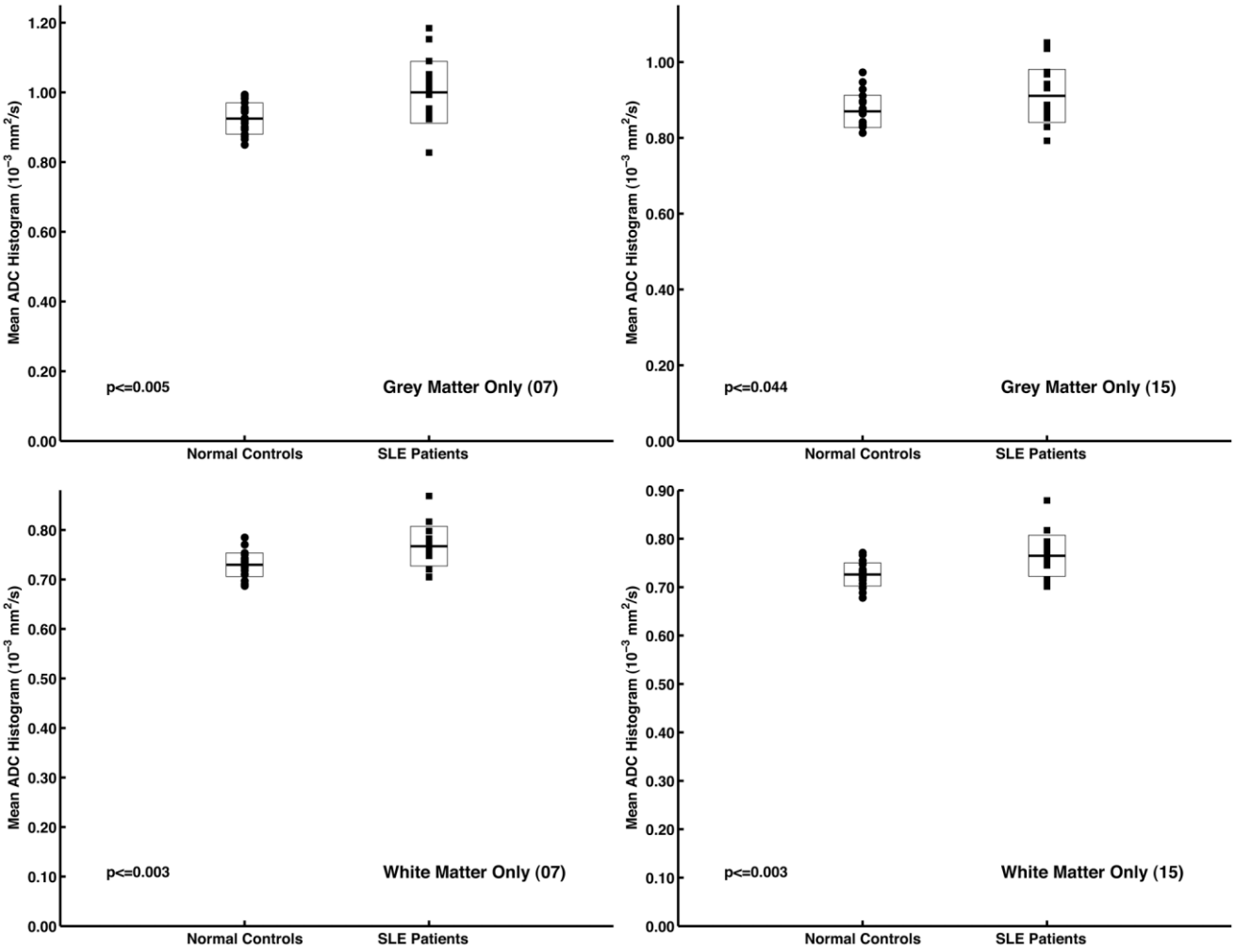


**Figure 7.** Individual mean values of ADC histograms for gray matter and white matter tissue, respectively, with increased neighborhood-like function. Left side for seven like-neighbors and right side for 15 like-neighbors. Boxes indicate ± SD about the mean.

decline in NAA is suggested to be a sign of neuronal loss, whereas an increase in the choline compounds can be assumed to be a sign of increased metabolic turnover/activity. These MRS findings, previously demonstrated in our patients (43), further support the theory of permanent axonal loss and associated demyelination.

The increased ADC values seen in the present study in the 17 NPSLE patients could be explained by reduced structural integrity with permanent loss of neurons and demyelination. This will allow the interstitial water molecules to move freely in a less restricted environment. This assumption is also suggested by others, with similar findings of abnormal ADC in NPSLE patients (24). If there is a breakdown of the myelin, as suggested by abnormal values of the metabolite choline seen in MR spectroscopy performed in some of our patients, the ADC value would also increase. Normally, the ADC values decrease by the restriction of motion in a particular direction. The myelin sheets form such a boundary and if they breakdown ADC will increase. The observation that there is increased ADC in white matter only, and that this observation is stable regardless of the neighborhood-like function, is consistent with a change in the myelin. Additionally, given that there appears to be no specific locale associated with the increased ADC observed in the white matter, this is a systemic effect. Using diffusion tensor imaging and the subsequent anisotropy measures in the future will provide for better evaluation of these hypotheses.

The observed increase in gray matter ADC appears somewhat dependent on the definition of a gray matter voxel. As the neighborhood-like function is made more stringent, the differences in mean ADC value between NPSLE patients and normal controls begins to diminish and, at the tightest definition of gray matter, the ADC difference loses significance. This could be due to some influence of partial voluming with CSF; however, at the mid-definition of gray matter, all ADC measures (mean, SD, skew, and kurtosis) remain significantly different between the NPSLE patients and normal controls. This result can be interpreted as consistent with inflammation and/or vasculitis of the gray matter. However, acquiring high-resolution 3D T1- or T2-weighted images in future studies will aid in addressing this issue.

Table 4
Histogram Statistical Results*

| Group | White-matter ADC | | Gray-matter ADC | | | |
|---|---|---|---|---|---|---|
| | Mean ($10^{-6}$ mm$^2$/second) | SD ($10^{-6}$ mm$^2$/second) | Mean ($10^{-6}$ mm$^2$/second) | SD ($10^{-6}$ mm$^2$/second) | Skew | Kurtosis |
| No "neighborhood-like" requirement | | | | | | |
| NPSLE | **768.6 ± 10.1** | 105.7 ± 4.4 | **1033.3 ± 24.3** | **268.3 ± 18.3** | **1.65 ± 0.19** | **10.53 ± 1.45** |
| Normals | **730.4 ± 5.3** | 101.1 ± 2.0 | **944.2 ± 10.9** | **210.5 ± 8.0** | **2.52 ± 0.07** | **16.57 ± 0.73** |
| *P* | **≤0.0020** | N.S. | **≤0.0022** | **≤0.0068** | **≤0.0003** | **≤0.0008** |
| "Neighborhood-like" value of at least seven required | | | | | | |
| NPSLE | **767.1 ± 10.0** | 104.3 ± 4.4 | **1000.1 ± 22.1** | **236.7 ± 15.4** | **1.30 ± 0.12** | **8.2 ± 0.80** |
| Normals | **729.6 ± 5.3** | 99.7 ± 2.1 | **924.9 ± 10.0** | **179.2 ± 6.5** | **1.86 ± 0.07** | **12.78 ± 0.48** |
| *P* | **≤0.0023** | N.S. | **≤0.0041** | **≤0.0018** | **≤0.00023** | **≤0.0001** |
| "Neighborhood-like" value of at least 15 required. | | | | | | |
| NPSLE | **764.7 ± 10.6** | 100.1 ± 4.8 | **910.6 ± 17.5** | **181.3 ± 16.0** | 0.98 ± 0.08 | 5.15 ± 0.25 |
| Normals | **726.1 ± 5.3** | 95.9 ± 2.2 | **869.8 ± 9.5** | **131.4 ± 5.0** | 1.04 ± 0.08 | 6.25 ± 0.60 |
| *P* | **≤0.0026** | N.S. | **≤0.0440** | **≤0.0063** | N.S. | N.S. |

*Summary of statistical findings of ADC histograms between NPSLE patients and normal controls. Values are derived from group mean, standard error is derived from group variance. Significant *P*-values are shown in bold.
N.S. = not significant.

One of the limitations with this study is that we have not performed specific brain volume segmentation for brain volume loss. However, only four of the 17 NPSLE patients finally evaluated in this study (patients 4, 7, and 10 where excluded as mentioned earlier) had brain atrophy, which was considered mild in two patients with only mild prominence of sulci over the convexity, slightly more then expected for patients age but without obvious/visible loss of gray matter, especially, and moderate in two patients. However, by constraining the definition of gray matter with the neighborhood-like function, and by further normalizing each subjects ADC histogram independently, issues of atrophy are mitigated. And, even with these tighter definitions of gray matter and white matter, we still observe statistically significant differences between groups.

Therefore, we are presently conducting such studies and are also combining the different available techniques such as MR spectroscopy and MR perfusion to be able to better understand and explain the underlying pathophysiology behind these changes seen in NPSLE patients.

Combining data from two separate sites can be problematic. To determine if observed differences in the ADC histograms between controls and patients are being driven by one of the imaging sites, we performed an explicit statistical comparison of ADC histograms of controls (21 controls from site one and nine controls from site two) between sites and the included patients in this study between sites. A Kolmogorov-Smirnov test statistic (44) was calculated between groups for whole brain, gray matter only, and white matter only. In each case the null hypothesis was accepted (i.e., ADC distributions are drawn from same parent sample), thus indicating nonsignificant difference between sites. Additionally, a Student's *t*-test statistic was calculated between sites for the two groups (controls and patients) separately for mean observed values of ADC. No statistically significant difference was found, again indicating that controls from either site are equivalent and that patients from either site are equivalent.

In conclusion, ADC histogram analysis demonstrated increased general diffusivity in the brain in NPSLE patients with acute neurological symptoms as compared with healthy normal controls. This finding suggests that in the brain parenchyma of NPSLE patients a loss of tissue integrity occurs and facilitates motility of free-water protons. Using segmented ADC histograms, this observed loss of tissue integrity has been observed in gray matter tissue and white matter tissue, separately. However, larger studies are needed to evaluate the present method for its value to study disease progression or its use in treatment control.

## REFERENCES


1. Kovacs J, Urowitz M, Gladman D. Dilemmas in neuropsychiatric lupus. Rheum Dis Clin N Am 1993;19:795–819.
2. Denburg SD, Behmann SA, Carbotte RM, Denburg JA. Lymphocyte antigens in neuropsychiatric systemic lupus erythematosus. Relationship of lymphocyte antibody specificities to clinical disease. Arthritis Rheum 1994;37:369–375.
3. ACR Ad Hoc Committee on Neuropsychiatric Lupus Nomenclature. The American College of Rheumatology nomenclature and case definitions for neuropsychiatric lupus syndromes. Arthritis Rheum 1999;42:599–608.
4. Wasserman BA, Stone JH, Hellman DB, Pomper MG. Reliability of normal findings on MR imaging for excluding the diagnosis of vasculitis of the central nervous system. AJR 2001;177:455–459.
5. Jennings JE, Sundgren PC, Attwood J, McCune J, Maly P. Value of brain MRI in SLE patients presenting with neurologic symptoms. Neuroradiology 2004;46:15–21.
6. Pomper M, Miller T, Stone J, Tidmore W, Hellman D. CNS vasculitis in autoimmune disease: MR imaging findings and correlation with angiography. AJNR Am J Neuroradiol 1999;20:75–85.
7. McCune J, MacGuire A, Aisen A, Gebarski S. Identification of brain lesions in neuropsychiatric systemic lupus erythematosus by magnetic resonance scanning. Arthritis Rheum 1988;31:159–166.
8. Jacobs L, Kinkel P, Costello PB, Alukal MK, Kinkel WR, Green FA. Central nervous system lupus erythematosus: the value of magnetic resonance imaging. J Rheumatol 1988;15:601–606.

9. Sibbitt WL Jr, Sibbitt RR, Griffey RH, Eckel C, Bankhurst AD. Magnetic resonance and computed tomographic imaging in the evaluation of acute neuropsychiatric disease in systemic lupus erythematosus. Ann Rheum Dis 1989;12:1014–1022.
10. Moseley M, Cohen Y, Kucharczyk J, et al. Diffusion-weighted MR-imaging of anisotropic water diffusion in cat central nervous system. Radiology 1990;176:439–445.
11. Le Bihan D. Molecular diffusion nuclear magnetic resonance imaging. Magn Reson Q 1991;7:1–30.
12. Bammer R. Basic principles of diffusion-weighted imaging. Eur J Radiol 2003;45:169–184.
13. Moseley ME, Kucharczyk J, Mintorovitch J, et al. Diffusion-weighted MR imaging of acute stroke: correlation with T2-weigthed and magnetic susceptibility-enhanced MR imaging in cats. AJNR Am J Neuroradiol 1990;11:423–429.
14. Lansberg MG, Norbash AM, Marks MP, Tong DC, Moseley ME, Albers GW. Advantages of adding diffusion-weighted magnetic resonance imaging to conventional magnetic resonance imaging for evaluating acute stroke. Arch Neurol 2000;57:1311–1316.
15. Larsson HBW, Thomsen C, Fredriksen J, Stubgaard M, Henriksen O. In vivo magnetic resonance diffusion measurements in the brain of patients with multiple sclerosis. Magn Reson Imaging 1992;10: 7–12.
16. Horsfield MA, Lai M, Webb S, et al. Apparent diffusion coefficients in benign and secondary progressive multiple sclerosis by nuclear magnetic resonance. Magn Reson Med 1996;36:393–400.
17. Christensen P, Gideon P, Thomsen C, Stubgaard M, Henriksen O, Larsson HBW. Increased water self-diffusion in chronic plaques and in apparently normal white matter in patients with multiple sclerosis. Acta Neurol Scand 1993;87:195–197.
18. Nakahara M, Ericsson K, Bellander BM. Diffusion-weighted MR and apparent diffusion coefficient in the evaluation of severe brain injury. Acta Radiol 2001;42:365–369.
19. Sundgren PC, Reinstrup P, Romner B, Holtas S, Maly P. Value of conventional, and diffusion- and perfusion weighted MRI in the management of patients with unclear cerebral pathology, admitted to the intensive care unit. Neuroradiology 2002;44:674–680.
20. Stadnik T, Chaskis C, Michotte A, et al. Diffusion-weighted MR imaging of intracerebral masses: comparison with conventional MR imaging and histologic findings. ANJR Am J Neuroradiol 2001;22: 969–976.
21. Kono K, Inoue Y, Nakayama K, et al.. The role of diffusion-weighted imaging in patients with brain tumors. AJNR Am J Neuroradiol 2001;22:1081–1088.
22. Sundgren PC, Edvardssson B, Holtas S. Serial investigation of perfusion disturbances and vasogenic oedema in hypertensive encephalopathy by diffusion and perfusion weighted imaging. Neuroradiology 2002;44:299–304.
23. Hinchey J, Chaves C, Applgnani B, et al. A reversible posterior leukoencephalopathy syndrome. N Engl J Med 1996;334:494–500.
24. Bosma GPTh, Huizinga TWJ, Mooijaart SP, van Buchem MA. Abnormal brain diffusivity in patients with neuropsychiatric systemic lupus erythematosus. AJNR Am J Neuroradiol 2003;24:850–854.
25. Wilson M, Morgan PS, Lin X, Turner BP, Blumhardt LD. Quantitative diffusion weighted magnetic resonance imaging, cerebral atrophy, and disability in multiple sclerosis. J Neurol Neurosurg Psychiatry 2001;70:318–322.
26. Wilson M, Trench CR, Morgan PS, Blumhardt LD. Pyramidal tract mapping by diffusion tensor magnetic resonance imaging in multiple sclerosis: improving correlations with disability. J Neurol Neurosurg Psychiatry 2003;74:203–207.
27. Tan E, Cohen A, Fries J, et al. The 1982 revised criteria for the classification of systemic lupus erythematosus. Arthritis Rheum 1982;25:1271–1277.
28. Jenkinson M, Bannister PR, Brady JM, Smith SM. Improved optimisation for the robust and accurate linear registration and motion correction of brain images. Neuroimage 2002;17:825–841.
29. Ashburner J, Friston KJ. Multi-modal image coregistration and partitioning—a unified framework. Neuroimage 1997;6:209–217.
30. Sibbitt Jr WL, Haseler LJ, Griffey RR, Friedman SD, Brooks WM. Neurometabolism of active neuropsychiatric lupus determined with proton MR spectroscopy. AJNR Am J Neuroradiol 1997;18: 1271–1277.
31. Hanly JG, Walsh NM, Sangalang V. Brain pathology in systemic lupus erythematosus. J Rheumatol 1992;19:732–741.
32. Johnson RT, Richardson EP. The neurological manifestations of systemic lupus erythematosus. Medicine (Baltimore) 1968;47:337–369.
33. Ellis SG, Verity MA. Central nervous system involvement in systemic lupus erythematosus; a review of neuropathological findings in 57 cases 1955–1977. Semin Arthritis Rheum 1979;8:212–221.
34. Zvaifler NJ, Bluestein HG. The pathogenesis of central nervous system manifestations of systemic lupus erythematosus. Arthritis Rheum 1982;25:862–866.
35. Pinching AJ, Travers RL. Hughes GR, Jones T, Moss S. Oxgygen-15 brain scanning for detection of cerebral involvement in systemic lupus erythematosus. Lancet 1978;1:898–900.
36. Kushner MJ, Chawluk J, Fazekas F, et al. Cerebral blood flow in systemic lupus erythematosus with and without cerebral complications. Neurology 1987;37:1596–1598.
37. Kovacs JA, Urowitz MB, Gladman DD, Zeman R. The use of single photon emission computerized tomography in neuropsychiatric SLE: a pilot study. J Rheumatol 1995;22:1247–1253.
38. Falconi F, De Cristofaro MT, Ermini M, et al. Regional cerebral blood flow in juvenile systemic lupus erythematosus: a prospective SPECT study. Single photon emission computed tomography. J Rheumatol 1998;25:583–588.
39. Kao CH, Lan JL, ChangLai SP, Liao KK, Yen RF, Chieng PU. The role of FDG-PET, HMPAO-SPECT and MRI in the detection of brain involvement in patients with systemic lupus erythematosus. Eur J Nucl Med 1999;26:129–134.
40. Bosma GPTh, Rood MJ, Huizinga TWJ, De Jong BA, Bollen ELEM, Van Buchem MA. Detection of cerebral involvement in patients with active neuropsychiatric systemic lupus erythematosus using magnetization transfer imaging. Arthritis Rheum 2000;43:2428–2436.
41. Brooks WM, Sabet A, Sibbitt Jr WL, et al. Neurochemistry of brain lesions determined by spectroscopic imaging in systemic lupus erythematosus. J Rheumatol 1997;24:2323–2329.
42. Chinn RJS, Wilkinson ID, Hall-Craggs MA, et al. Magnetic resonance imaging of the brain and cerebral proton spectroscopy in patients with systemic lupus erythematosus. Arthritis Rheum 1997;40:36–46.
43. Sundgren PC, Jennings J, Attwood TJ, McCune W, Gebarski S, Maly P. MRI and 2D-MR CSI spectroscopy of the brain in the evaluation of patients with acute onset of neuropsychiatric systemic lupus erythematosus. Neuroradiology 2005;47:576–585.
44. Kanji GK. 100 statistical tests. Thousand Oaks, CA: Sage Publications; 1993. 68 p.